

Mono- τ Signatures at the LHC Constrain Explanations of B -decay Anomalies

Admir Greljo,¹ Jorge Martin Camalich,^{1,2,3} and José David Ruiz-Álvarez⁴

¹Theoretical Physics Department, CERN, 1 Esplanade des Particules, 1211 Geneva 23, Switzerland

²Instituto de Astrofísica de Canarias, C/ Vía Láctea, s/n E38205—La Laguna, Tenerife, Spain

³Universidad de La Laguna, Departamento de Astrofísica, 38200—La Laguna, Tenerife, Spain

⁴Instituto de Física, Universidad de Antioquia, A.A. 1226 Medellín, Colombia



(Received 10 December 2018; published 5 April 2019)

We investigate the crossing-symmetry relation between $b \rightarrow c\tau\bar{\nu}$ decay and $b\bar{c} \rightarrow \tau\bar{\nu}$ scattering to derive direct correlations of new physics in semitauonic B -meson decays and the mono-tau signature at the LHC ($pp \rightarrow \tau_n X + \text{MET}$). Using an exhaustive set of effective operators and heavy mediators we find that the current ATLAS and CMS data constrain scenarios addressing anomalies in B decays. Pure tensor solutions, completed by leptoquark, and right-handed solutions, completed by W'_R or leptoquark, are challenged by our analysis. Furthermore, the sensitivity that will be achieved in the high-luminosity phase of the LHC will probe *all* the possible scenarios that explain the anomalies. Finally, we note that the LHC is also competitive in the $b \rightarrow u$ transitions and bounds in some cases are currently better than those from B decays.

DOI: [10.1103/PhysRevLett.122.131803](https://doi.org/10.1103/PhysRevLett.122.131803)

Introduction.—Branching fractions of semitauonic B -meson decays, measured through the ratios $R_{D^{(*)}} = \Gamma(B \rightarrow D^{(*)}\tau\nu)/\Gamma(B \rightarrow D^{(*)}\ell\nu)$ (with $\ell = e$ or μ), appear to be enhanced with respect to the standard model (SM) by roughly thirty percent, with a global significance of $\sim 4\sigma$ [1–11]. If this is due to new physics (NP), its mass scale is expected to be not far above the TeV scale (see, e.g., [12]). The most immediate question is whether such NP is already ruled out by the existing high- p_T searches and, if not, what the road map is for its direct discovery.

From a bottom-up perspective the NP interpretation of the $R_{D^{(*)}}$ anomalies involves two different aspects, (i) new dynamics (i.e., degrees of freedom), and (ii) the flavor structure. Both aspects are relevant when it comes to identifying correlated effects in other observables such as weak hadron or τ decays, electroweak precision observables, and high- p_T LHC signatures (see, e.g., [13]).

The Lorentz structure of the effective operators that describe the effects of the hypothesized heavy mediators at low energies can be discriminated by using $b \rightarrow c\tau\nu$ decay data alone [14–24]. On the other hand, most flavor data are consistent with the SM, which suggests that such NP must couple mainly to the third generation of quarks and leptons [13,25–32]. However, in general, and without the guidance of a theory of flavor, models addressing the anomalies have some freedom in the way they implement couplings in

flavor space. All this complicates defining conclusive tests in other weak hadron decays or clear direct-search strategies at the LHC.

The aim of this Letter is to discuss and explore in detail the phenomenology of a collider signature that should be produced at the LHC by any model addressing the $R_{D^{(*)}}$ anomalies with new heavy mediators. The main idea, illustrated in Fig. 1, is that regardless of the Lorentz and flavor structure of the NP, crossing symmetry univocally connects the $b \rightarrow c\tau\bar{\nu}$ decay and the $b\bar{c} \rightarrow \tau\bar{\nu}$ scattering processes [14,33–36]. As we demonstrate below, the analysis of $pp \rightarrow \tau\nu X$ at the LHC already excludes broad classes of models addressing the anomalies and provides a “no-lose theorem” for the direct discovery of NP at the LHC, in case the $R_{D^{(*)}}$ anomalies were confirmed in the future. Furthermore, these searches simultaneously constrain operators involving semitauonic $b \rightarrow u$ transitions with bounds that are currently competitive, or even better, than those obtained in B decays.

Effective field theory.—We start with an effective field theory (EFT) of NP in semitauonic $b \rightarrow u_i$ transitions (with u_i up or charm quarks) valid at energies $\sim \mathcal{O}(m_b)$ [37,38],

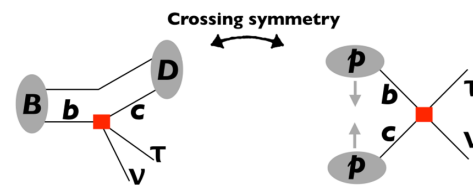


FIG. 1. Illustration of the complementarity in $b \rightarrow c\tau\nu$ transitions as measured in B -meson decays and inclusive production of $\tau + \text{MET}$ of high- p_T LHC.

Published by the American Physical Society under the terms of the [Creative Commons Attribution 4.0 International license](https://creativecommons.org/licenses/by/4.0/). Further distribution of this work must maintain attribution to the author(s) and the published article's title, journal citation, and DOI. Funded by SCOAP³.

$$\begin{aligned}
 \mathcal{L}_{\text{eff}} \supset & -\frac{2V_{ib}}{v^2} [(1 + \epsilon_L^{ib})(\bar{\tau}\gamma_\mu P_L \nu_\tau)(\bar{u}_i \gamma^\mu P_L b) \\
 & + \epsilon_R^{ib}(\bar{\tau}\gamma_\mu P_L \nu_\tau)(\bar{u}_i \gamma^\mu P_R b) + \epsilon_T^{ib}(\bar{\tau}\sigma_{\mu\nu} P_L \nu_\tau)(\bar{u}_i \sigma^{\mu\nu} P_L b) \\
 & + \epsilon_{S_L}^{ib}(\bar{\tau} P_L \nu_\tau)(\bar{u}_i P_L b) + \epsilon_{S_R}^{ib}(\bar{\tau} P_L \nu_\tau)(\bar{u}_i P_R b)] + \text{H.c.}, \quad (1)
 \end{aligned}$$

where subindices label quark flavor in the mass basis, V_{ij} are the Cabibbo-Kobayashi-Maskawa (CKM) matrix elements, $P_{L,R}$ are the chiral projectors, $\sigma^{\mu\nu} = i/2[\gamma^\mu, \gamma^\nu]$, and we have used $v \approx 246$ GeV as the electroweak symmetry breaking (EWSB) scale. With this normalization, the Wilson coefficients (WCs) scale as $\epsilon_\Gamma \sim v^2/\Lambda^2$, where Λ is the characteristic scale of NP [39]. Light right-handed neutrinos can be added to Eq. (1) with the replacements $P_L \rightarrow P_R$ in the leptonic currents and $\epsilon_\Gamma \rightarrow \tilde{\epsilon}_\Gamma$ in labeling the WCs. None of these operators interfere with the SM for vanishing neutrino masses.

In order to connect this EFT to NP with a typical scale $\Lambda \gg v$, one needs to switch first to another EFT that is invariant under $SU(2)_L \times U(1)_Y$ and is built using the full field content of the SM [40,41]. Without specifying the flavor structure, we focus on the collider signature that stems exclusively from four-fermion operators giving $\bar{c}b\bar{\nu} \nu$ in the fermion mass basis, which are the ones directly linked to $R_{D^{(*)}}$. Finally, when connecting the values of the WCs at $\mu = m_b$ to those at $\mu = \Lambda$, one needs to account for the rescaling and mixing effects induced by the renormalization group evolution produced by SM radiative corrections [42–47].

At low energies, these operators induce semitauonic B decays, as shown in Fig. 1, left. The characteristic $(V - A)$ structure remaining in the $\Lambda \rightarrow \infty$ limit incarnates the SM contribution, whereas different combinations of these operators have been found to accommodate the $R_{D^{(*)}}$ anomalies [48–50]. A sample of the preferred NP solutions is shown in Table I.

At high energies, these operators contribute to $pp \rightarrow \tau \nu X$ at the LHC, as shown in Fig. 1, right. Schematically, the ratio of NP and SM cross sections for this process, at energies $\sqrt{s} \gg M_W$ and leading order in QCD, reads

$$\frac{\sigma_{\text{NP}}}{\sigma_{\text{SM}}} \sim \frac{\sum_i \mathcal{L}_{ib} \otimes |V_{ib}|^2 \frac{s}{v^4} (\alpha_\Gamma |\epsilon_\Gamma^{ib}|^2)}{\mathcal{L}_{ud} \otimes |V_{ud}|^2 \frac{s}{v^4} (\frac{M_W^2}{s})^2}, \quad (2)$$

where the sum over flavors refers to the up and charm quark in Eq. (1) and is convoluted by the luminosity functions \mathcal{L}_{ij} containing the corresponding parton distribution functions (PDF). The SM cross section is given by the W^\pm exchange while in the NP one α_Γ is an operator-dependent factor stemming from the trace of the corresponding Dirac structures (e.g., $\alpha_L = 1$) [38]. The sensitivity to NP in $b \rightarrow u_i$ comes from the quadratic dependence on the WCs, while contributions linear in the WCs are only relevant in

TABLE I. Fitted values of the WCs at $\mu = m_b$ of the EFT Lagrangian of Eq. (1) with errors at 1σ for semitauonic $b \rightarrow c$ transitions fitted to the current values of $R_{D^{(*)}}$. For each scenario only the WCs mentioned are fitted while others are set to 0 (see also Refs. [48–50]). For the theoretical inputs we follow Ref. [22].

Left-handed	Tensor	Scalar tensor	Right handed
ϵ_L^{cb}	ϵ_T^{cb}	$\epsilon_{S_L}^{cb}$	$\tilde{\epsilon}_R^{cb}$
0.11(2)	0.37(1)	0.18(7)	-0.042(10)
			0.48(6)

the interference with the SM contribution involving up and down quarks [33,51].

At first glance, one might conclude that effects in $b \rightarrow u_i$ are negligible when compared with the dominant SM production from $u\bar{d}$, $d\bar{u}$ fusion, which is PDF and CKM favored. However, in the high- p_T tails above the EWSB scale, the SM amplitude unitarizes while the EFT one keeps growing. Interestingly, the energy enhancement in the tails is large enough to compensate for the aforementioned suppressions leading to bounds competitive to B decays. Finally, the absence of interference effects implies that the collider signature is sensitive only to the Lorentz structure (vector, scalar, or tensor) and not to the chirality of the partonic currents.

To perform our numerical collider studies we use the FEYNRULES [52], MADGRAPH [53,54], PYTHIA [55] and DELPHES [56] simulation chain to generate samples of the inclusive process $pp \rightarrow \tau_h X + \text{MET}$. The signal, as a function of the WCs, is compared to the m_T distributions of W' searches reported in this channel by ATLAS (36.1 fb^{-1}) [57] and CMS (35.9 fb^{-1}) [58] assuming Poissonian probabilities for the events in each bin [59]. In addition, we perform a sensitivity study for the LHC after run 2 (150 fb^{-1}) and after the HL-LHC phase (3 ab^{-1}), assuming that the systematic uncertainties of the SM background scale with luminosity as $\delta/N \sim 1/\sqrt{N}$ [60]. A detailed description of the numerical analysis can be found in the Supplemental Material [61].

In Table II we show the results of our NP collider analysis in terms of the cb four-fermion operators. The fits to the two collaborations differ mainly because ATLAS has a slight excess of events in the m_T distribution, whereas the one of CMS is systematically consistent with the SM. The most remarkable result shown in this table is that, combining the analysis of the two sets of data, we arrive at a sensitivity to NP that is, indeed, competitive to the one achieved in B decays. In fact, the collider data pose already a challenge to some of the possible explanations to the $R_{D^{(*)}}$ anomaly. To make this discussion clearer, we compare in Fig. 2 the results from the fits to $R_{D^{(*)}}$ shown in Table I with the ones obtained from the collider analysis. The tensor and right-handed solutions are excluded at more than 2σ with

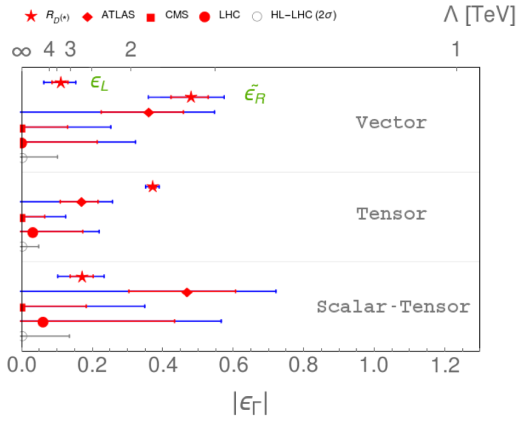


FIG. 2. 1σ (red) and 2σ (blue) ranges on the absolute value of the WCs of semitauonic cb transitions at $\mu = m_b$.

the current data, while the HL-LHC will probe the two remaining scenarios in Table I.

A caveat in this analysis concerns the range of convergence of the expansion in powers of (s/Λ^2) implied by the EFT. This manifests, for instance, in the pathological behavior of the cross section, Eq. (2), for $\sqrt{s} \gg \Lambda$, leading to the upper bound $\Lambda \lesssim 9$ TeV by means of unitarity arguments [12]. In the upper horizontal axis of Fig. 2 we show the bounds in terms of the NP scale defined as $\Lambda = v/\sqrt{|V_{cb}||\epsilon_\Gamma|}$. These bounds are within the range of m_T reported by the experiments. The bins most sensitive to NP turn out to be those in $0.7 \text{ TeV} \lesssim m_T \lesssim 1.8 \text{ TeV}$; removing the tail of the distribution above that region has a minimal impact, of $\lesssim 10\%$, on the bounds (see also Supplemental Material [61]). Therefore, the EFT analysis should retain its validity for mediators above this scale.

For scenarios with lighter NP, the EFT study is invalid and one needs to do the analysis in terms of the particular UV completions of the operators. The possibilities in terms of mediators are also quite limited, reducing to the tree-level exchange of either new colorless vector (W') [28,66–72] and scalar (H^\pm) [73–77] particles in the s channel, or leptoquarks in the t channel [27,48,50,78–99]. We do not consider extra Higgs bosons because they are in conflict with bounds from the decay $B_c \rightarrow \tau\nu$ [14,16].

The leptoquark completion.—Leptoquarks (LQs) carrying different quantum numbers (or combinations thereof) can produce all the operators in Eq. (1) [27,48,50,78–99]

TABLE II. 2σ upper bounds for the absolute value of the WCs of semitauonic cb transitions at $\mu = m_b$.

Data set	Vector	Scalar	Tensor
ATLAS (36.1 fb $^{-1}$)	0.55	0.93	0.26
CMS (35.9 fb $^{-1}$)	0.25	0.45	0.12
LHC combined	0.32	0.57	0.16
LHC (150 fb $^{-1}$)	0.21	0.37	0.10
HL-LHC	0.10	0.17	0.05

(we use same notation as in Refs. [100,101]). Our analysis involve (i) the scalar LQ $S_1 = (\bar{3}, 1, 1/3)$ producing vector-current (left-handed or right-handed) solutions, (ii) the S_1 producing the scalar-tensor solution, (iii) the S_1 combined with the scalar LQ $R_2 = (3, 2, 7/6)$ to achieve a tensor solution by adjusting the masses $M_{S_1} = M_{R_2}$, and (iv) the vector LQ $U_1 = (3, 1, 2/3)$ leading also to the vector-current scenarios. All in all, we study four different LQ models, accounting for a total of six different NP solutions to the $R_{D^{(*)}}$ anomalies.

We simulate the signals scanning the LQ masses in the range 0.75 to 5 TeV and, for a given mass, we derive upper bounds on the product of LQ couplings to c and b quarks. In all the models we find that the bounds on the coupling-mass plane of the LQ are approximately equal to those derived from the EFT solutions they incarnate for masses $\gtrsim 2\text{--}3$ TeV. Solutions with lower masses are, nevertheless, being cornered by the aforementioned direct searches. Therefore, the conclusions for the LQ are very similar to the EFT analysis: The two LQ $S_1 - R_2$ scenario is excluded by more than 2σ in all the mass range. Right-handed solutions [50,99] with S_1 and U_1 are also excluded by $\gtrsim 2\sigma$ except for masses below 2 TeV. This mass range is accessible with $\sim 150 \text{ fb}^{-1}$ expected to be gathered after run 2 of the LHC. Finally, the left-handed (S_1 or U_1) and scalar-tensor (S_1) scenarios are not being probed yet but will be covered at the HL-LHC for almost the full mass range. We show in Fig. 3, left, a coupling-mass plot for the U_1 vector LQ illustrating our results and conclusions ($\mathcal{L} \supset g_c \bar{c} \gamma_\mu P_{L,R} \nu U_1^\mu + g_b \bar{b} \gamma_\mu P_{L,R} \tau U_1^\mu$). Similar plots for the other LQ have been presented elsewhere [102].

The W' completion.—The left-handed solution can be completed by a new massive spin-1 real $SU(2)_L$ triplet vector, $W'_L = (\mathbf{1}, \mathbf{3}, 0)$ [28] (see also [67,82,103]). The neutral component of the triplet (a Z' boson nearly degenerate to W'^\pm) leads to dangerous tree-level effects in neutral meson mixing. The flavor structure that keeps the contribution in $\Delta F = 2$ observables under control unavoidably predicts a $\mathcal{O}(V_{cb}^{-1})$ enhancement in $b\bar{b} \rightarrow Z' \rightarrow \tau^+ \tau^-$. A recast of the ATLAS $\tau^+ \tau^-$ search with 3.2 fb^{-1} at 13 TeV, performed in Ref. [104], already cuts deep into the model's perturbative parameter space explaining the anomaly, requiring the Z' to be a rather wide resonance. A second class of models involves a complex vector, $SU(2)_L$ singlet with a hypercharge, $W'_R = (\mathbf{1}, \mathbf{1}, +1)$, and a relatively light right-handed neutrino that induces the right-handed solution to $R_{D^{(*)}}$ [70,71] (see also [105,106]). Explicit UV models introduce a Z' boson with flavor violating effects completely decoupled from $R_{D^{(*)}}$ due to the lack of $SU(2)_L$ relations.

The relevant W' interactions are defined as $\mathcal{L} \supset g_{bc} \bar{c} \gamma^\mu P_{L,R} b W'_\mu + g_{\tau\nu} \bar{\nu} \gamma^\mu P_{L,R} \tau W'_\mu + \text{H.c.}$, where the chirality is inaccessible in our present analysis. We perform simulations using the same specifications as for the EFT, for several W' masses in the range 0.5 to 3.5 TeV and

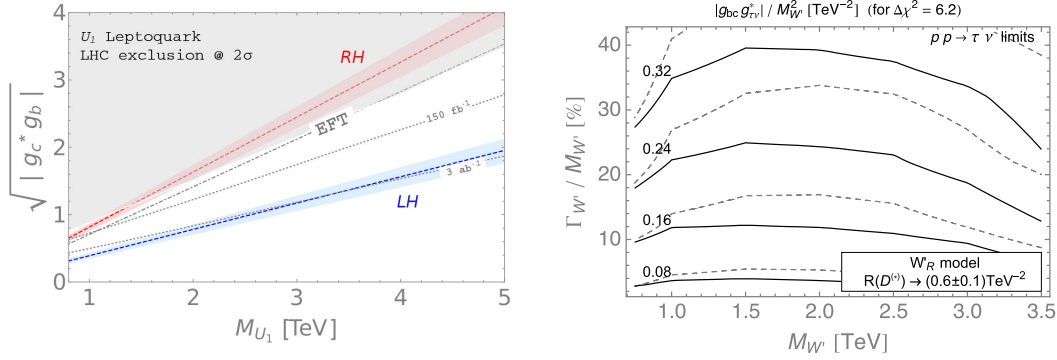


FIG. 3. Bounds on representative explicit models that address the $R_{D^{(*)}}$ anomalies. Left: The U_1 vector leptoquark (LQ). Right: A potentially broad W' gauge boson. See the main text for details.

different total width hypotheses. Besides including experimental systematics and the SM theory uncertainties, we also estimate the uncertainty on the signal prediction stemming from the higher-order QCD corrections and PDF determination. These uncertainties combined in quadrature range from roughly 10% (30%) for $m_{W'} = 1$ TeV (3 TeV)—see also Supplemental Material [61]. For a given mass and width combination, we set an upper limit on the product of the two couplings in the $W'bc$ and $W'\tau\nu$ vertices, and confront it with the fit results from $R_{D^{(*)}}$.

Note that this procedure is rather general, and it does not require one to specify any details of other W' decay modes. This choice of parameters is suitable for the interpretation of the perturbativity of the model. Very wide resonances indicate the loss of predictivity and here we investigate up to $\Gamma_{W'} \lesssim 0.5M_{W'}$. Our results, shown in Fig. 3 (right) in solid (dashed) for observed (expected), exclude the W'_R models in the perturbatively calculable parameter space explaining the anomaly, $|g_{bc}g_{\tau\nu}^*|/M_{W'}^2 \approx (0.6 \pm 0.1)$ TeV⁻². This quantity is $\approx (0.14 \pm 0.03)$ TeV⁻² for the left-handed solution, which is, however, scrutinized by the $Z' \rightarrow \tau^+\tau^-$ searches at the LHC [104].

A potential caveat could be the loss of sensitivity in the low W' mass region as the signal tends to hide in the large SM background. Robust lower limits of $\gtrsim 100$ GeV on a new electrically charged gauge boson from the LEP experiments are significantly improved by the electroweak $pp \rightarrow W^+W^-$ pair-production process at the LHC [107]. Another promising direction to close this window is to study $pp \rightarrow \tau\nu$ searches at previous pp collision energies [107]. Search strategies in this region could include requiring a b tag in the final jets [36]. Some sensitivity is expected also in the top quark decays [108].

The semitauonic $b \rightarrow u$ transitions.—NP models addressing $R_{D^{(*)}}$ are expected to contribute to semitauonic transitions other than $b \rightarrow c$, and to neutral-current processes via $SU(2)_L$ symmetry (e.g., for the LQ or W'_L). Focusing on the charged currents and their impact on the mono-tau signal at the LHC, we conclude from Eq. (2) that additional flavor structures can only enhance the $pp \rightarrow \tau\nu$

signal [109]. Thus, the bounds obtained above are conservative in the sense that they can only be stronger in realistic models of NP.

We explore this issue by repeating our analysis for $b \rightarrow u$ operators in the EFT. These are particularly interesting transitions because they are typically affected by NP addressing $R_{D^{(*)}}$. Experimentally, branching fractions of $B \rightarrow \tau\nu$ have been measured, showing a slight excess over the SM at $\sim 1.5\sigma$, while there is only an upper limit on the semitauonic decay $B^0 \rightarrow \pi^-\tau^+\nu$. In Table III, we show the bounds on the different structures that are obtained from $pp \rightarrow \tau\nu X$ at the LHC, assuming that these are the only active flavor entries. The limits on the ub WCs are roughly a factor 2 worse than for the cb ones, which is the result of the CKM suppression $(|V_{ub}|/|V_{cb}|)^2$ partially compensated by the larger PDFs of the up quark, cf., Eq. (2). Nonetheless, these are competitive with those obtained from B decays. In particular, LHC bounds are currently better than the ones derived from $B^0 \rightarrow \pi^-\tau^+\nu$ [110], $-1.25 \lesssim \epsilon_T^{ub} \lesssim 0.57$ and $-1.75 \lesssim \epsilon_{S_L}^{ub} + \epsilon_{S_R}^{ub} \lesssim 0.94$ at 2σ , using the form factors from lattice QCD calculations [111,112].

Conclusions and discussion.—We have discussed in detail the consequences of the univocal connection between the semitauonic B decays and the $pp \rightarrow \tau\nu X + \text{MET}$ signature at the LHC given by crossing symmetry, cf., Fig. 1. Our key findings can be summarized as follows: First, the current data at 13 TeV on W' searches, consisting of roughly ~ 36 fb⁻¹ per collaboration, are already sensitive to NP scenarios addressing the $R_{D^{(*)}}$ anomalies. Pure tensor solutions, completed by LQ, and right-handed solutions, completed by W'_R or LQ, are excluded at more than 2σ for most of masses. Second, the sensitivity that is achieved by extrapolating through the HL-LHC phase will probe all the possible scenarios that explain the anomalies. Therefore mono-tau searches can provide a no-lose theorem or “the ultimate test” for the confirmation of such NP at the LHC. Third, the LHC is also competitive in the $b \rightarrow u$ transitions and bounds on some NP scenarios are currently better than those from B decays. This illustrates the impact, and

TABLE III. 2σ upper bounds for the absolute value of the WCs of semitauonic ub transitions at $\mu = m_b$.

Data set	Vector	Scalar	Tensor
LHC combined	0.72	1.23	0.34
LHC (150 fb ⁻¹)	0.48	0.84	0.23
HL-LHC	0.21	0.37	0.10

complementarity with low-energy experiments, that a program of high-precision measurements at the LHC can have in flavor physics.

In our analysis, the sensitivity to NP comes mainly from the m_T bins around ~ 1 TeV, while the EFT provides a good description of explicit models (with the exception of light W'). The implied constraints are difficult to avoid by more elaborate model building (compared to, e.g., [104]). Finally, significant improvements of the present analysis are possible in the future. For instance, exploiting τ_h charge asymmetries, rapidity distribution, and polarization could help improve the signal over background discrimination. Another avenue would be to consider adding data from the leptonic tau decays. A detailed study of these aspects and their impact on the sensitivity will be presented elsewhere [107].

We thank Martin Gonzalez-Alonso, David Marzocca, and Christos Vergis for useful discussions. J. M. C. acknowledges support from the Spanish MINECO through the ‘‘Ram3n y Cajal’’ Grant No. RYC-2016-20672. J. D. R.-A. gratefully acknowledges the support of COLCIENCIAS, the Administrative Department of Science, Technology, and Innovation of Colombia and Sostenibilidad-UdeA.

-
- [1] J. P. Lees *et al.* (BABAR Collaboration), *Phys. Rev. Lett.* **109**, 101802 (2012).
- [2] J. P. Lees *et al.* (BABAR Collaboration), *Phys. Rev. D* **88**, 072012 (2013).
- [3] M. Huschle *et al.* (Belle Collaboration), *Phys. Rev. D* **92**, 072014 (2015).
- [4] Y. Sato *et al.* (Belle Collaboration), *Phys. Rev. D* **94**, 072007 (2016).
- [5] R. Aaij *et al.* (LHCb Collaboration), *Phys. Rev. Lett.* **115**, 111803 (2015); **115**, 159901(A) (2015).
- [6] S. Hirose *et al.* (Belle Collaboration), *Phys. Rev. Lett.* **118**, 211801 (2017).
- [7] S. Hirose *et al.* (Belle Collaboration), *Phys. Rev. D* **97**, 012004 (2018).
- [8] R. Aaij *et al.* (LHCb Collaboration), *Phys. Rev. Lett.* **120**, 171802 (2018).
- [9] R. Aaij *et al.* (LHCb Collaboration), *Phys. Rev. D* **97**, 072013 (2018).
- [10] R. Aaij *et al.* (LHCb Collaboration), *Phys. Rev. Lett.* **120**, 121801 (2018).
- [11] S. Aoki *et al.*, *Eur. Phys. J. C* **77**, 112 (2017).
- [12] L. Di Luzio and M. Nardecchia, *Eur. Phys. J. C* **77**, 536 (2017).
- [13] D. Buttazzo, A. Greljo, G. Isidori, and D. Marzocca, *J. High Energy Phys.* **11** (2017) 044.
- [14] R. Alonso, B. Grinstein, and J. Martin Camalich, *Phys. Rev. Lett.* **118**, 081802 (2017).
- [15] A. Datta, S. Kamali, S. Meinel, and A. Rashed, *J. High Energy Phys.* **08** (2017) 131.
- [16] A. G. Akeroyd and C.-H. Chen, *Phys. Rev. D* **96**, 075011 (2017).
- [17] C.-T. Tran, M. A. Ivanov, J. G. Korner, and P. Santorelli, *Phys. Rev. D* **97**, 054014 (2018).
- [18] U. Nierste, S. Trine, and S. Westhoff, *Phys. Rev. D* **78**, 015006 (2008).
- [19] S. Fajfer, J. F. Kamenik, and I. Nisandzic, *Phys. Rev. D* **85**, 094025 (2012).
- [20] Y. Sakaki, M. Tanaka, A. Tayduganov, and R. Watanabe, *Phys. Rev. D* **91**, 114028 (2015).
- [21] Z. Ligeti, M. Papucci, and D. J. Robinson, *J. High Energy Phys.* **01** (2017) 083.
- [22] R. Alonso, A. Kobach, and J. Martin Camalich, *Phys. Rev. D* **94**, 094021 (2016).
- [23] R. Alonso, J. M. Camalich, and S. Westhoff, *Phys. Rev. D* **95**, 093006 (2017).
- [24] P. Asadi, M. R. Buckley, and D. Shih, *Phys. Rev. D* **99**, 035015 (2019).
- [25] B. Bhattacharya, A. Datta, D. London, and S. Shivashankara, *Phys. Lett. B* **742**, 370 (2015).
- [26] S. L. Glashow, D. Guadagnoli, and K. Lane, *Phys. Rev. Lett.* **114**, 091801 (2015).
- [27] R. Alonso, B. Grinstein, and J. Martin Camalich, *J. High Energy Phys.* **10** (2015) 184.
- [28] A. Greljo, G. Isidori, and D. Marzocca, *J. High Energy Phys.* **07** (2015) 142.
- [29] F. Feruglio, P. Paradisi, and A. Pattori, *Phys. Rev. Lett.* **118**, 011801 (2017).
- [30] F. Feruglio, P. Paradisi, and A. Pattori, *J. High Energy Phys.* **09** (2017) 061.
- [31] J. Kumar, D. London, and R. Watanabe, *Phys. Rev. D* **99**, 015007 (2019).
- [32] F. Feruglio, P. Paradisi, and O. Sumensari, *J. High Energy Phys.* **11** (2018) 191.
- [33] T. Bhattacharya, V. Cirigliano, S. D. Cohen, A. Filipuzzi, M. Gonzalez-Alonso, M. L. Graesser, R. Gupta, and H.-W. Lin, *Phys. Rev. D* **85**, 054512 (2012).
- [34] M. Gonzalez-Alonso and J. Martin Camalich, *J. High Energy Phys.* **12** (2016) 052.
- [35] W. Altmannshofer, P. S. Bhupal Dev, and A. Soni, *Phys. Rev. D* **96**, 095010 (2017).
- [36] M. Abdullah, J. Calle, B. Dutta, A. Flrez, and D. Restrepo, *Phys. Rev. D* **98**, 055016 (2018).
- [37] W. D. Goldberger, arXiv:hep-ph/9902311.
- [38] V. Cirigliano, J. Jenkins, and M. Gonzalez-Alonso, *Nucl. Phys.* **B830**, 95 (2010).
- [39] Only one tensor operator is allowed because $(\bar{\tau}\sigma_{\mu\nu}P_{L\nu})(\bar{u}_i\sigma^{\mu\nu}P_R b) = 0$.
- [40] W. Buchmuller and D. Wyler, *Nucl. Phys.* **B268**, 621 (1986).
- [41] B. Grzadkowski, M. Iskrzynski, M. Misiak, and J. Rosiek, *J. High Energy Phys.* **10** (2010) 085.

- [42] E. E. Jenkins, A. V. Manohar, and M. Trott, *J. High Energy Phys.* **10** (2013) 087.
- [43] E. E. Jenkins, A. V. Manohar, and M. Trott, *J. High Energy Phys.* **01** (2014) 035.
- [44] R. Alonso, E. E. Jenkins, A. V. Manohar, and M. Trott, *J. High Energy Phys.* **04** (2014) 159.
- [45] J. Aebischer, M. Fael, C. Greub, and J. Virto, *J. High Energy Phys.* **09** (2017) 158.
- [46] M. Gonzalez-Alonso, J. Martin Camalich, and K. Mimouni, *Phys. Lett. B* **772**, 777 (2017).
- [47] E. E. Jenkins, A. V. Manohar, and P. Stoffer, *J. High Energy Phys.* **01** (2018) 084.
- [48] M. Freytsis, Z. Ligeti, and J. T. Ruderman, *Phys. Rev. D* **92**, 054018 (2015).
- [49] S. Bhattacharya, S. Nandi, and S. Kumar Patra, [arXiv:1805.08222](https://arxiv.org/abs/1805.08222).
- [50] D. J. Robinson, B. Shakya, and J. Zupan, *J. High Energy Phys.* **02** (2019) 119.
- [51] V. Cirigliano, A. Falkowski, M. Gonzalez-Alonso, and A. Rodriguez-Sanchez, [arXiv:1809.01161](https://arxiv.org/abs/1809.01161).
- [52] A. Alloul, N. D. Christensen, C. Degrande, C. Duhr, and B. Fuks, *Comput. Phys. Commun.* **185**, 2250 (2014).
- [53] J. Alwall, M. Herquet, F. Maltoni, O. Mattelaer, and T. Stelzer, *J. High Energy Phys.* **06** (2011) 128.
- [54] J. Alwall, R. Frederix, S. Frixione, V. Hirschi, F. Maltoni, O. Mattelaer, H. S. Shao, T. Stelzer, P. Torrielli, and M. Zaro, *J. High Energy Phys.* **07** (2014) 079.
- [55] T. Sjstrand, S. Ask, J. R. Christiansen, R. Corke, N. Desai, P. Ilten, S. Mrenna, S. Prestel, C. O. Rasmussen, and P. Z. Skands, *Comput. Phys. Commun.* **191**, 159 (2015).
- [56] J. de Favereau, C. Delaere, P. Demin, A. Giammanco, V. Lematre, A. Mertens, and M. Selvaggi (DELPHES 3 Collaboration), *J. High Energy Phys.* **02** (2014) 057.
- [57] M. Aaboud *et al.* (ATLAS Collaboration), *Phys. Rev. Lett.* **120**, 161802 (2018).
- [58] A. M. Sirunyan *et al.* (CMS Collaboration), *Phys. Lett.* (to be published).
- [59] G. Cowan, K. Cranmer, E. Gross, and O. Vitells, *Eur. Phys. J. C* **71**, 1554 (2011); **73**, 2501(E) (2013).
- [60] Projected performance of Higgs analyses at the HL-LHC for ECFA 2016, CERN Technical Report No. CMS-PAS-FTR-16-002, 2017.
- [61] See Supplemental Material at <http://link.aps.org/supplemental/10.1103/PhysRevLett.122.131803> for technical details of our analysis. In particular, we describe in detail the parameters of our collider simulations comparing them to the official ones reported by ATLAS and CMS. We also include a careful analysis of the range of transverse mass most sensitive to the effect of the effective-field-theory operators and of the theoretical uncertainties stemming from next-to-leading-order QCD corrections and pdfs, which includes Refs. [62–65].
- [62] B. Diaz, M. Schmaltz, and Y.-M. Zhong, *J. High Energy Phys.* **10** (2017) 097.
- [63] I. Dorner and A. Greljo, *J. High Energy Phys.* **05** (2018) 126.
- [64] M. Tanabashi *et al.* (Particle Data Group), *Phys. Rev. D* **98**, 030001 (2018).
- [65] J. Butterworth *et al.*, *J. Phys. G* **43**, 023001 (2016).
- [66] S. M. Boucenna, A. Celis, J. Fuentes-Martin, A. Vicente, and J. Virto, *Phys. Lett. B* **760**, 214 (2016).
- [67] E. Megias, M. Quiros, and L. Salas, *J. High Energy Phys.* **07** (2017) 102.
- [68] X.-G. He and G. Valencia, *Phys. Lett. B* **779**, 52 (2018).
- [69] S. Matsuzaki, K. Nishiwaki, and R. Watanabe, *J. High Energy Phys.* **08** (2017) 145.
- [70] A. Greljo, D. J. Robinson, B. Shakya, and J. Zupan, *J. High Energy Phys.* **09** (2018) 169.
- [71] P. Asadi, M. R. Buckley, and D. Shih, *J. High Energy Phys.* **09** (2018) 010.
- [72] S. Iguro, Y. Omura, and M. Takeuchi, [arXiv:1810.05843](https://arxiv.org/abs/1810.05843).
- [73] M. Tanaka, *Z. Phys. C* **67**, 321 (1995).
- [74] A. Celis, M. Jung, X.-Q. Li, and A. Pich, *J. High Energy Phys.* **01** (2013) 054.
- [75] A. Celis, M. Jung, X.-Q. Li, and A. Pich, *Phys. Lett. B* **771**, 168 (2017).
- [76] S. Iguro and K. Tobe, *Nucl. Phys.* **B925**, 560 (2017).
- [77] S. Fraser, C. Marzo, L. Marzola, M. Raidal, and C. Spethmann, *Phys. Rev. D* **98**, 035016 (2018).
- [78] Y. Sakaki, R. Watanabe, M. Tanaka, and A. Tayduganov, *Phys. Rev. D* **88**, 094012 (2013).
- [79] R. Barbieri, G. Isidori, A. Pattori, and F. Senia, *Eur. Phys. J. C* **76**, 67 (2016).
- [80] S. Fajfer and N. Košnik, *Phys. Lett. B* **755**, 270 (2016).
- [81] X.-Q. Li, Y.-D. Yang, and X. Zhang, *J. High Energy Phys.* **08** (2016) 054.
- [82] R. Barbieri, C. W. Murphy, and F. Senia, *Eur. Phys. J. C* **77**, 8 (2017).
- [83] D. Becirevic, S. Fajfer, N. Konik, and O. Sumensari, *Phys. Rev. D* **94**, 115021 (2016).
- [84] A. Crivellin, D. Mller, and T. Ota, *J. High Energy Phys.* **09** (2017) 040.
- [85] Y. Cai, J. Gargalionis, M. A. Schmidt, and R. R. Volkas, *J. High Energy Phys.* **10** (2017) 047.
- [86] N. Assad, B. Fornal, and B. Grinstein, *Phys. Lett. B* **777**, 324 (2018).
- [87] L. Di Luzio, A. Greljo, and M. Nardecchia, *Phys. Rev. D* **96**, 115011 (2017).
- [88] M. Bordone, C. Cornella, J. Fuentes-Martin, and G. Isidori, *Phys. Lett. B* **779**, 317 (2018).
- [89] R. Barbieri and A. Tesi, *Eur. Phys. J. C* **78**, 193 (2018).
- [90] D. Marzocca, *J. High Energy Phys.* **07** (2018) 121.
- [91] U. Aydemir, D. Minic, C. Sun, and T. Takeuchi, *J. High Energy Phys.* **09** (2018) 117.
- [92] A. Greljo and B. A. Stefanek, *Phys. Lett. B* **782**, 131 (2018).
- [93] M. Blanke and A. Crivellin, *Phys. Rev. Lett.* **121**, 011801 (2018).
- [94] M. Bordone, C. Cornella, J. Fuentes-Martin, and G. Isidori, *J. High Energy Phys.* **10** (2018) 148.
- [95] D. Beirevi, I. Dorner, S. Fajfer, D. A. Faroughy, N. Konik, and O. Sumensari, *Phys. Rev. D* **98**, 055003 (2018).
- [96] L. Di Luzio, J. Fuentes-Martin, A. Greljo, M. Nardecchia, and S. Renner, *J. High Energy Phys.* **11** (2018) 081.
- [97] A. Angelescu, D. Bečirević, D. A. Faroughy, and O. Sumensari, *J. High Energy Phys.* **10** (2018) 183.
- [98] J. Heeck and D. Teresi, *J. High Energy Phys.* **12** (2018) 103.
- [99] A. Azatov, D. Barducci, D. Ghosh, D. Marzocca, and L. Ubaldi, *J. High Energy Phys.* **10** (2018) 092.

- [100] W. Buchmuller, R. Ruckl, and D. Wyler, *Phys. Lett. B* **191**, 442 (1987); **448**, 320(E) (1999).
- [101] I. Dorner, S. Fajfer, A. Greljo, J. F. Kamenik, and N. Konik, *Phys. Rep.* **641**, 1 (2016).
- [102] Talk by A. Greljo, Workshop on high-energy implications of flavor anomalies (2018).
- [103] S. M. Boucenna, A. Celis, J. Fuentes-Martin, A. Vicente, and J. Virto, *J. High Energy Phys.* **12** (2016) 059.
- [104] D. A. Faroughy, A. Greljo, and J. F. Kamenik, *Phys. Lett. B* **764**, 126 (2017).
- [105] M. Carena, E. Megas, M. Quros, and C. Wagner, *J. High Energy Phys.* **12** (2018) 043.
- [106] K. S. Babu, B. Dutta, and R. N. Mohapatra, *J. High Energy Phys.* **01** (2019) 168.
- [107] A. Greljo, J. Martin Camalich, and J. Ruiz-Alvarez (to be published).
- [108] J. F. Kamenik, A. Katz, and D. Stolarski, *J. High Energy Phys.* **01** (2019) 032.
- [109] With the exception of contributions in the valence ud flavor entry that we do not consider because it is tightly constrained by τ decays [51].
- [110] P. Hamer *et al.* (Belle Collaboration), *Phys. Rev. D* **93**, 032007 (2016).
- [111] J. A. Bailey *et al.* (Fermilab Lattice, MILC Collaborations), *Phys. Rev. D* **92**, 014024 (2015).
- [112] J. A. Bailey *et al.* (Fermilab Lattice, MILC Collaborations), *Phys. Rev. Lett.* **115**, 152002 (2015).